Topology of 2-dim Expanding Slow Hydrogen-Air Flames in Cylindrical Horizontal Hele-Shaw Cell

Filippov A.E.[1)], Nikolaev I.I.[1)], Denisenko V.P.[1)],
Gubernov V.V. [2)], Plaksin V.Yu. [4)], Moskalev P.V. [3)], Kirillov I.A. [1)]
[1)] National Research Centre "Kurchatov Institute", Moscow, Russia
[2)] P.N. Lebedev Physical Institute of the Russian Academy of Sciences, Moscow, Russia
[3)] Voronezh State Technical University, Voronezh, Russia
[4)] Kintech Lab Ltd, Moscow, Russia

1 Introduction

Velocity and topology of the rection front are two key characteristics both the slow and fast flames, which can freely propagate in the hydrogen-air gas mixtures either in 3dim or in 2dim environment. Despite of the extensive studies (for example - theoretical [1-3], experimental [4-11] and computational [12-19]), focused on reaction front structure and its stability for the slow, laminar flames in hydrogen-air mixtures, the clear answers on the following questions are still absent: 1) How many distinct (from topological viewpoint) types of the slow flames can be discriminated in the hydrogen-air mixtures within their flammability concentration range (4 – 75 vol.% H_2)? 2) What are the archetypical microstructural elements (basic constituents), which inherent to specific flame front macroscopic morphology (at given mixture stoichiometry) ? 3) What are the quantitative (measurable or computed) metrics – macroscopic and microscopic - for a topology-based classification of the slow flames ? Goals of this report are – 1) to answer on the posed questions for the specific case – quasi 2-dim cylindrical expansion of the slow flames in closed axisymmetric horizontal Hele-Shaw cell and 2) to provide the direct experimental evidences on the basic morphotypes and to propose a preliminary set of the metrics for classification and quantitative characterisation of the distinct, freely propagating, slow hydrogen-air flames.

2 Experimental

For systematic exploration of the topologically different hydrogen-air flames morphotypes we used Hele-Shaw cell, described in [20]. Additional video camera was used – Evercam 2000-8-C - with resolution 1280×860 pixels and frame speed at max resolution 2000 fps. A whole flammability concentration range (from 4 to 75 vol.% H_2) have been studied to extend and complement of the previous experiments [20] in ultra-lean mixtures (< 12 vol.% H_2). We used just horizontal, cylindrical cell with axisymmetric ignition for two reasons – 1) to minimize impact of gravity and buoyance, 2) to provide opportunity for cylindrical expansion of flame for explicit and easy-to-comprehend (in comparison to 3dim cases [4,5]) demonstration of the topological features of the flames during their

Correspondence to: kirillov.igor@gmail.com

ontogenetic evolution. Observation of some of these features is hindered in the Hele-Shaw cells with rectangular geometry and side ignition.

3 Results

3.1 Flame front morphotypes (macroscopic)

With a sequential increase of the initial hydrogen concentration (from 4 to 75 vol.% H_2) in hydrogen-air gas mixtures under normal conditions (300 K, 1 atm), only six distinct (from topological and dynamic viewpoint) macroscopic morphotypes of the cylindrically expanding, laminar flames have been recorded (see Figure 1). The first three morphotypes (self-quenching flame balls, ray-like and dendritic) form a first family of the discrete (non-coherent) flames, which are characterized by a system of the multiple discrete reaction fronts, separated by the unreacted zones. Last three morphotypes (cellular, petal- and ring-like) constitute a second family of the flames with the continuous single reaction fronts, which differ by macroscopic wrinkling and microscopic structure of flame brush.

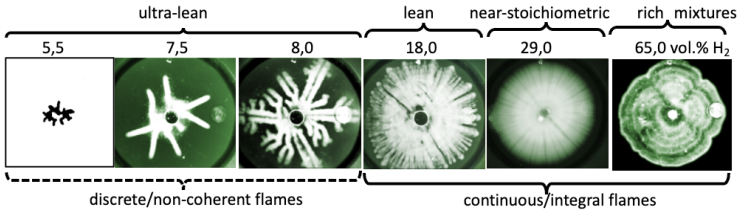

Figure 1: Six topologically and dynamically distinct macroscopic morphotypes of the hydrogen-air flames in horizontal Hele-Shaw cell (4.5 mm thickness): 1) self-quenching flame balls, 2) ray-like, 3) dendritic, 4) cellular, 5) petal-like, 6) ring-like.

The observed quasi-2dim flame morphotypes have their 3dim analogues listed in Table 1.

Table 1: Basic topologically different slow, laminar, quasi-2dim flames and their 3dim counterparts.

№	families	quasi-2dim experiments		3dim experiments				stoichiom.
		cylindrical geometry	rectangular geometry	g=9,8 m/sec^2		μg		
1	non-coherent/ discrete flames	ray-like [20] [1)]	[10] [2)]	raspberry-like	[21]	isolated flame balls	[5]	ultra-lean
2		dendritic [20] [1)]	[10] [2)]	vortex-like	[21]	cellular flamelets	[5]	ultra-lean
3	contin./ integral flames	cellular [20, 17]	[9,10] [3)]	cellular deflagration	[6,8, 21,22]	cellular deflagration	[5]	lean
4		petal-like (this work) [17]	[9]	unwrinkled deflagration	[6, 8, 22]	n/a		near-stoich.
5		ring-like (this work)	n/a	pulsating deflagration	[13]	n/a		rich

Notes: Computational studies: [1)] in [18]; [2)] in [14,16]; [3)] in [14,15]

3.2 Meso- and micro-scopic reaction front patterns (elementary building blocks)

3.2.1 Isolated Drifting Flame Balls (one- and two-headed)

The first four macroscopic morphotypes (self-quenching, ray-like, dendritic and cellular) are defined by interaction and dynamics of a system of the isolated Drifting Flame Balls. Their two basic microscopic structures (one- or two-headed), studied computationally in [18, 20]. In the weakest near-limit ultra-lean mixtures (see Figure 2-1 and 2-2), flames were formed by a set of practically non-interacting self-quenched or self-sustaining DFBs. Each DFB propagates in a separate angular sector (shown by orange lines). Number of the angular sectors is equivalent to the number of the first-generation DFBs, formed due to primary bifurcation [24] of the pre-flame kernel, caused by the diffusional-thermal instability. The higher hydrogen concentration the higher number of sectors. Despite stochastic nature of the DFBs formation, the 1- and 2-headed DFBs propagate alternately in the adjacent sectors (see Figure 2-2 and 2-3). Isolated one-headed DFBs are either self-quenched in near-limit mixtures (see Figure 2-1) or self-sustained (Figure 2-2). In stronger mixtures both 1- and 2-headed DFBs have self-branching [24] nature. They can propagate as a stable [18] entities or can transform (bifurcate and merge) into each other during higher order bifurcations (see Figure 2-3) of the DFB themselves. At Figure 2-3 the specific features for ultra-lean stoichiometry are shown: 1) bifurcation of one 1H-DFB into two 1H-DFB and subsequent synchronic propagation, 2) formation of a strongly interacting DFBs, whose evolution results in formation of a topologically stable macroscopic pattern - Flame Branch (propagating in a single angular sector, marked by ABC). It consists of - 1) one leading ("edge") first generation ("parent") central 2H-DFB and 2) the a few "child" (secondary, tertiary and quaternary…) collateral 1H-DFBs, branched from the left and right components of the two "parent" 1-headed DFB. The higher hydrogen concentration the higher number of the one-headed "child" 1H-DFBs in a single Flame Branch.

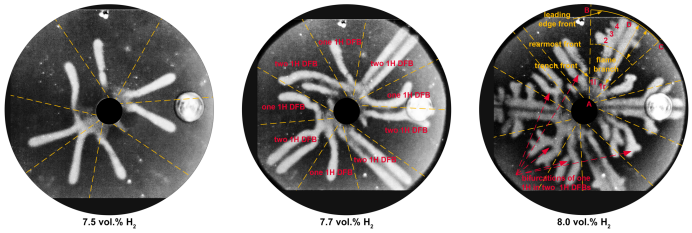

Figure 2: (1 and 2) One-headed Drifting Flame Balls as elementary constituents of the non-coherent flames with ray-like and dendritic morphotypes. (3) Transitions from one 1H-DFB into two 1H-DFBs.

3.2.2 Systems of Strongly Interacting Drifting Flame Balls (Flame Branches with Triangle Leading Edge)

In the stronger (ultra-lean and lean) mixtures three effects take place. Total number of the sectors and the self-branching DFBs is increased (Figure 2-3 and 3-1). DFBs start to interact with each other via higher order bifurcations of the DFBs themselves. First generation (shown by 1 at Figure 2-3) of the DFB, formed due to primary bifurcation of the pre-flame kernel, undergone the secondary, tertiary and quaternary bifurcations. Each subsequent bifurcations occurs at finite distance along the first-generation DFB pathway. A set of the mutually interacting DFBs, which propagate within a single angular sector, form a Flame Branch. Usually, macroscopic leading edge (shown by yellow continuous line at Figures 2-3, 3-1 and 3-2) of the Flame Branch is a 2-headed DFB. Reaction occurs also at a few separated DFBs, allocated along the mesoscopic envelops, shown by orange curves at Figure 2-3, 3-1 and 3-2. Distance from edge to rearmost reaction front (shown by dashed yellow lines) can be thought of as a first (macroscopic) geometrical characteristic - "thickness" (dashed yellow bidirectional arrows) of the flame brushes in the dendritic, cellular, petal- and ring-like flame morphotypes. Second (macroscopic) intrinsic characteristics both for the non-coherent and continuous flames is a distance (dotted yellow bidirectional

arrows) from cusp location (dotted yellow curve) to the leading-edge front – flame trench depth. Third (mesoscopic) characteristic is an angle between two tangents (blue lines) to mesoscopic envelops, which can be regarded as a metrics of overall curvature of the flame branches. Fourth and fifth (microscopic) metrics are – local curvatures of the leading ("parent") 2-headed DFB and the "child" 1H-DFBs, which belong to selected flame branch. Sixth macroscopic metric – tortuosity (wrinkling for continuous and lacunarity for discrete flames) of the leading-edge front. For wrinkled flames it's reasonable to use a fractal dimension. The increase of initial hydrogen concentration results in the following changes - thicknesses of flame brush become smaller, the flame trench depth become higher, the angle is become higher (mesoscopic curvature of flame branch is lowering) and the local curvatures of the DFBs become higher.

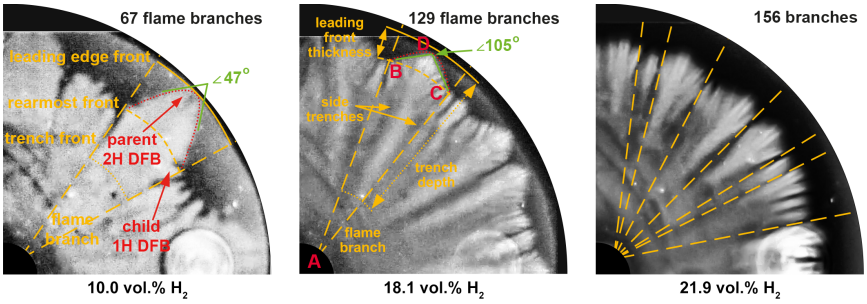

Figure 3: Branches of the interacting Drifting Flame Balls as elementary constituents of the flames with cellular morphotype (triangular leading-edge front).

3.2.3 Systems of interconnected segments of the nearly-plane intact deflagration fronts (flame branches with trapezoidal leading edge)

In the continuous/intact flames, the flame branches for the petal-like (in near-stoichiometric mixtures) and ring-like (in rich mixtures) morphotypes are consist of the connected segments (see Figure 4) of the deflagration reaction fronts, appropriately, with trapezoid and ring-like morphologies and divided by a trench with finite width.

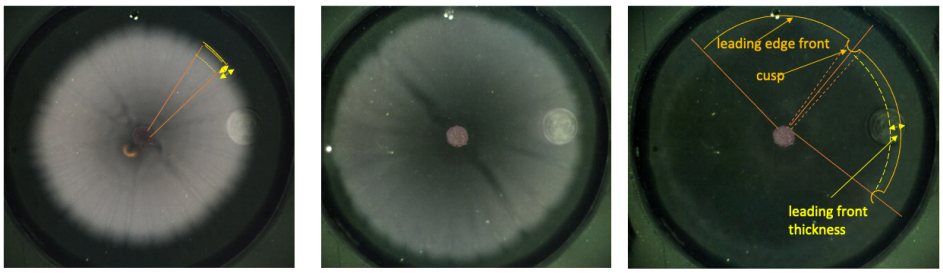

Figure 4: Segments of the deflagration fronts, divided by trenches with finite thickness, as elementary constituents of the flames with petal- and ring-like morphotype.

Both morphotypes are characterized by a with nearly-plane local curvature. Difference between them is the following. In the near-stoichiometric mixtures the combustion completeness (Figure 5) and velocity of reaction front are high, so water steam is condensing uniformly throughout (Figure 4-1 and 4-2) all space between leading edge front and central point of ignition. In the rich mixtures (Figure 4-3) the combustion completeness and front velocity are small and water steam is visible only for a thin ring-like reaction front. In both morphotypes two adjacent segments are divide by trench of finite width and depth, comparable with radius of the Hele-Shaw cell. Additional studies (in IR and UF ranges) are

necessary for detailed description the microstructure of the cusps (in cellular) and the trenches (petal- and ring-like) in the continuous flames with different morphotypes.

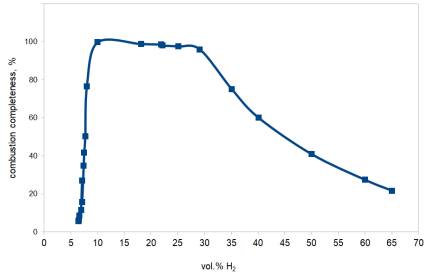

Figure 5: Combustion completeness vs initial stoichiometry (vol.% H2).

4 Conclusions

Experimental data on slow hydrogen-air flames topology were compiled from the previously published works from three viewpoints – 1) flame propagation symmetry (spherical, cylindrical, plane), 2) gravity/buoyancy impact (the Earth and microgravity conditions), 3) mixture stoichiometry. Systematic experiments in horizontal cylindrical Hele-Shaw cell were performed to close the existing gaps in understanding of the slow flame topologies within a 4 - 75 vol.% H_2 concentration range. It was observed that at macroscopic level only two basic families of slow hydrogen-air flames exist within flammability range of the hydrogen-air premixed mixtures, namely, non-coherent (discrete) flames and continuous (intact) flames. Flames mesoscopic constituents (flame branches) from both families cylindrically expand in the appropriate angle sectors. Number of these sectors is defined by diffusional-thermal or Darrieus-Landau instabilities of the pre-flame kernel, which is dominant for a given mixture stoichiometry. Within each sector a single flame branch is evolving. First flame family consists of two morphotypes - ray-like and dendritic. Each flame branch in non-coherent flames consist of a system of the elementary constituents (stable microscopic patterns), namely, multiple, discrete, locally spherical reaction fronts (Drifting Flame Balls), which interact (bifurcate, merge) with each other with different mode and intensity. Second flame family includes three morphotypes – cellular, petal- and ring-like. Flame branch in continuous cellular morphotype is also composed of the system of Drifting Flame Balls. In contrast with dendritic morphotype the leading-edge reaction front in cellular morphotype is continuous and have triangular shape. Flame branches in petal- and ring-like morphotype are composed of the segments of the locally planar Deflagration Flames with different tortuosity of the leading-edge front. Two adjacent branches are separated by either a pin-point cusp (in cellular morphotype) or by trench with finite width (in petal- and ring-like morphotypes). Six quantitative characteristics are proposed as a preliminary set of the metrics for comprehensive, evidence-based classification and quantitative characterisation of the topologically distinct, freely propagating, slow hydrogen-air flames.

Reference

[1] Ronney P.D., Sivashinsky G.I. (1989). A theoretical study of propagation and extinction of nonsteady spherical flame fronts. SIAM J. Appl. Math. 49(4): 1029-1046.

[2] Minaev S, Kagan L, Joulin G, Sivashinsky G. (2001) On self-drifting flame balls. Combustion Theory and Modeling. 5:609-622.

[3] Sanchez A., Williams F.A. (2014). Recent advances in understanding of flammability characteristics of hydrogen, Progress in Energy and Combustion Science, 41:1-55.

[4] Mitani T., Williams F.A. (1980). Studies of cellular flames in hydrogen-oxygen- nitrogen mixtures. Combust Flame. 39:169-190.

[5] Ronney P.D. (1998). Understanding combustion processes through microgravity research. Proc Combust. Inst. 27:2485-2506.

[6] Tse S.D., Zhu D.L., Law C.K. (2000). Morphology and burning rates of expanding spherical flames in H2/O2/inert mixtures up to 60 atmospheres. Proc. Combust. Inst. 28:1793-1800.

[7] Jomaas G., Law C.K. (2010). Observation and regime classification of pulsation patterns in expanding spherical flames. Phys Fluids. 22:124102.

[8] Sun Z.Yu., Li G.X., Li H.M., Zhai Yy., Zhou Z.H. (2014). Buoyant Unstable Behavior of Initially Spherical Lean Hydrogen-Air Premixed Flames. Energies. 7: 4938-4956.

[9] Wongwiwat J., Gross J., Ronney P.D. (2015). Flame propagation in narrow channels at varying Lewis number. Technical Report, 25th ICDERS. Paper No. 258.

[10] Veiga-López F., Kuznetsov M., Martínez-Ruiz D., Fernández-Tarrazo E., Grune J., Sánchez-Sanz M. (2020). Unexpected propagation of ultra-lean hydrogen flames in narrow gaps. Phys. Rev.Lett.124:174501.

[11] Grune J., Sepert K., Kuznetsov M., Jordan T. (2021). Experimental investigation of unconfined spherical and cylindrical flame propagation in hydrogen-air mixtures. Int. J. Hydrogen Energy. 46(23):12487-12496.

[12] Wu M.S., Ronney P.D., Colantonio R.O., van Zandt D.M. (1999). Detailed numerical simulation of flame ball structure and dynamics. Combust Flame 116:387-97.

[13] Christiansen, E. W., Law, C. K. & Sung, C. J. 2001. Steady and pulsating propagation and extinction of rich hydrogen/air flames at elevated pressures. Combust. Flame 124, 35–49.

[14] Fernandez-Galisteo D., Kurdyumov V.N., Ronney P.D. (2017). Analysis of premixed flame propagation between two closely-spaced parallel plates. Combustion and Flame. 190:133-145.

[15] Berger L., Kleinheinz K., Attili A., Pitsch H. (2018). Characteristic patterns of thermodiffusively unstable premixed lean hydrogen flames. Proc. Comb. Inst. 37:1879-1886.

[16] D. Martínez-Ruiz, F. Veiga-López, D. Fernández-Galisteo, V.N. Kurdyumov, M. Sánchez-Sanz (2019). The role of conductive heat losses on the formation of isolated flame cells in Hele-Shaw chambers. Combustion and Flame. 209:187-199.

[17] Gu G., Huang J., Han W., Wang C. (2021). Propagation of hydrogen-oxygen flames in Hele-Shaw cells. Int. J. Hydrogen Energy. 46: 12009-12015.

[18] Lu Z., Li J. (2021). Dynamics of flame rings in a thermally-conductive narrow channel: numerical experiment. Comb. Theory and Modeling 25:1158-1174.

[19] Dominguez A., Matrinez-Ruiz D., Snache-Sanz M. (2022) Stable circular and double-cell lean hydrogen-air premixed flames in quasi two-dimensional channels. Proc. Comb. Institute

[20] Denisenko V.P., et.al. (2021). Critical Morphological Phenomena during Ultra-Lean Hydrogen-Air Combustion in Closed Horizontal Hele-Shaw Cell, Proc. ICHS2021, paper 128.

[21] Anikin N.B., Kirillov I.A., (2022). Experimental Study of Early-Stage Dynamics of the Ascending and Descending Laminar Hydrogen-Air Flames in Vertical Closed Rectangular Tube. ICDERS2022. Paper 183.

[22] GraVent facility - shadowgraphy recordings database
https://www.epc.ed.tum.de/td/forschung/ddt/database/homogeneous-h2-air-mixtures/